# THE APPLICATION OF THE NORMALIZED VASICEK METHOD TO NONABSORBING SINGLE VAPOR-DEPOSITED LAYERS ON GLASS CARRIERS

Jürgen Rassow



Translation of "Die Anwendung des normierten Vasicek-Verfahrens bei nichtabsorbierenden Einfachaufdampfschichten auf Glasträgern", Zeitschrift für Physik. Vol. 170, 1962, pp. 376 - 392.

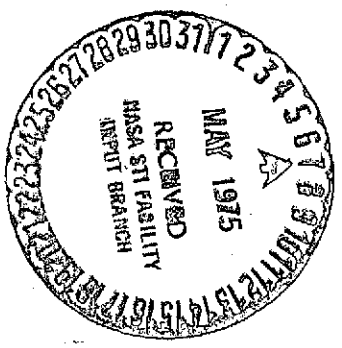


NATIONAL AERONAUTICS AND SPACE ADMINISTRATION
WASHINGTON, D. C. 20546 APRIL 1975

STANDARD TITLE PAGE

| 1. Report No. NASA TT F-16,261 | 2. Government Accession No. | 3. Recipient's Catalog No. |
|---|---|---|
| 4. Title and Subtitle: Application of the normalized Vasicek method to nonabsorbing single vapor-deposited layers on glass carriers. | | 5. Report Date: April 1975 |
| | | 6. Performing Organization Code |
| 7. Author(s): J. Rassow | | 8. Performing Organization Report No. |
| | | 10. Work Unit No. |
| 9. Performing Organization Name and Address: SCITRAN, Box 5456, Santa Barbara, CA 93108 | | 11. Contract or Grant No. NASw-2483 |
| | | 13. Type of Report and Period Covered: Translation |
| 12. Sponsoring Agency Name and Address: National Aeronautics and Space Administration, Washington, D.C. 20546 | | 14. Sponsoring Agency Code |

15. Supplementary Notes

Translation of "Die Anwendung des normierten Vasicek-Verfahrens bei nichtabsorbierenden Einfachaufdampfschichten auf Glastragern", Zeitschrift für Physik. Vol. 170, 1962, pp. 376 - 392.

16. Abstract

The author has modified Vasicek's polarimetric theory to a graphic method for determination of optical constants of thick homogeneous films on glass carriers. The method is verified for single layers deposited by heating salts. The kind of salt determines the gradient of the refractive index. This gradient and the state of the glass surface are responsible for deviations from the theoretical curves. A suitable method has been found for determining the refractive index and the thickness of the deposited film. In a modified form the method can also be used for inhomogeneous films.

| 17. Key Words (Selected by Author(s)) | 18. Distribution Statement: Unclassified - Unlimited | | |
|---|---|---|---|
| 19. Security Classif. (of this report): Unclassified | 20. Security Classif. (of this page): Unclassified | 21. No. of Pages: 24 | 22. Price |

# THE APPLICATION OF THE NORMALIZED VASICEK METHOD TO NONABSORBING SINGLE VAPOR-DEPOSITED LAYERS ON GLASS CARRIERS

Jürgen Rassow

## §1. Introduction

The modified Vasicek method [2] described in a previous publication [1] and brought to a normalizable form provides for the graphic evaluation of homogeneous dielectric layers on glass supports having no inherent natural transition layer. Vasicek [3] attempted to meet this condition by choosing freshly polished glass as the support. This seemed to him to have the least transition layers. / 376*

No systematic experimental test of the method has yet been carried out; and, especially, no investigation has been made of the consequences of layer inhomogeneities and stronger initial transition layers on the glass supports. Thus, the Vasicek evaluation method [1] should be tested by systematic measurements with various vapor-deposited layers from the following viewpoints: / 377

1. Consideration of the periodicities of the measurement curves, required in the theoretical Part I.
2. Comparison of the results of the measurements with three light wavelengths on the same layers.
3. Comparison of layers of the same material on glass supports with different refractive indices.

---

* Numbers in the margin indicate pagination in the original foreign text.

4. Comparison of the results obtained with polarized light and interference microscopy on the same layers.

## §2. The Theoretical Curves with Homogeneous Single Layers on Different Layer Supports

In order to get an indea of the measurements to be expected, let us first determine the theoretical values which one should obtain for the measurements,* using the massive values for refractive indices according to Table 1 ($\lambda$ = 5461 Å) on the basis of the families of curves from Part I in Figures T3, T7 and T9.

TABLE 1. MASSIVE VALUES FOR REFRACTIVE INDICES OF THE VAPOR-DEPOSITED SUBSTANCES ACCORDING TO LANDOLT-BORNSTEIN.

| $\lambda$ [Å] | 4358 | 5461 | 5780 |
|---|---|---|---|
| LiF . . . . | 1,3967 | 1,3929 | 1,3919 |
| NaCl . . . | 1,5603 | 1,5474 | 1,5450 |
| LiCl . . . . | | | 1,66 |
| AgCl . . . | 2,131 | 2,077 | 2,064 |
| AgBr . . . | 2,354 | 2,273 | 2,265 |

Figure 1 shows such curves for NaCl layers on three glasses. The following statements can be applied:

1. Because of the specialization on the polarization angle, $\varphi_p$, the decision whether the layer refractive index, $n_s$, is greater or smaller than that of the support, n, can be made only from the sign ($\alpha$) [See Eq. (T23)[1]].
2. $\alpha$ begins and ends with the value $\alpha_n = 0$ at the limits of the periods. In the center of the periods it passes

---

* The definitions are chosen exactly as they are introduced in Part I and explained. Thus, $\alpha$ is the azimuth of the major axis of the reflected vibration ellipse with respect to the normal to the plane of incidence, and $\tan\gamma$ is the ellipticity.

through a maximum. The period limits are given by $x = 0° + z \cdot 360°$, and the centers by $x = 180° + z \cdot 360°$, where z indicates the number of periods.

3. The γ curves begin and end also with the value $\gamma_n = 0$ at the period limits; but already in the first half-period they pass through an extreme with the sign of (α). At the center of the period they pass through zero and repeat the curve of the first half, reflected at $z = 0.5$, but with the sign of (-α). / 378

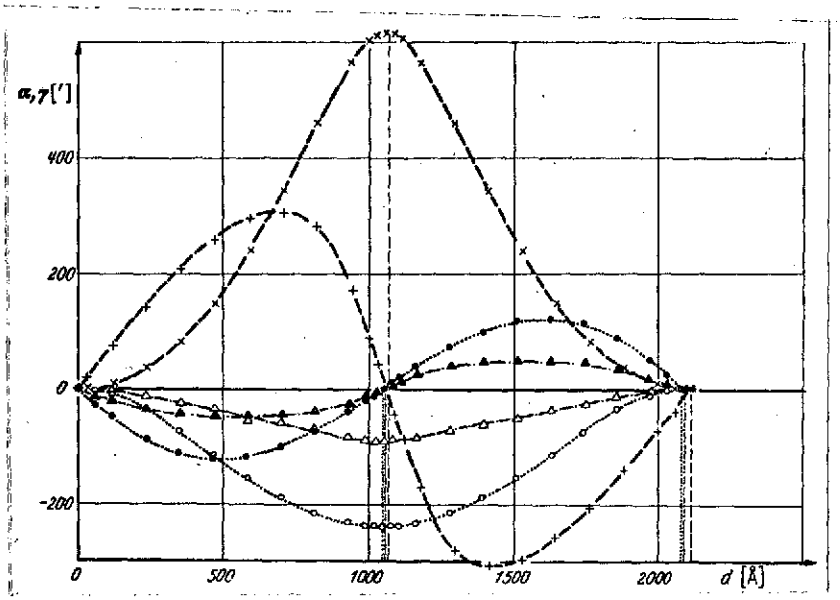


Figure 1. Theoretical α and γ curves for NaCl layers on prisms with n = 1.4678 ( o····o: α; •····•: γ ); n = 1.5188 ( ▲—·—▲: α; ▲—·—▲: γ ) and n = 1.7234 ( ×——×: α; +——+: γ ).

4. The zeros for the α and γ curves at the period limits, the maximum, $\alpha_m$, of the α curves, and the zero passage of the γ curves from the region with the sign of (α) to the region with the sign of (-α) all coincide exactly for the same layer thickness.

5. The extremes, $\gamma_m$, of the $\gamma$ curves have almost exactly the same height difference as the $\alpha$ extremes.
6. a) At the points $\partial\alpha/\partial d=0$, $\gamma$ always has a non-zero derivative. b) At the points $\partial\gamma/\partial d=0$, the second derivative of $\alpha$ vanishes; i. e., this is an inflection point.
7. It follows from 6a and 6b that the magnitude of the effect on the layer data, $n_s$ and d, alternates periodically between $\alpha$ and $\gamma$ and simultaneously takes on the two opposing extremes.
8. In the center of the period, because $\gamma = 0$, then according to Equation (T1), $\alpha=\alpha_m^0=\psi_{max}$, so that here it is particularly easy to take the values for $n_s$ or $n_f$, respectively, from the $\psi_{max}$ curves of Figure T8 or Figures T3 or T7.
9. The period length, L, depends on the support refractive index only in the second approximation through the changed polarization angle according to Equation (T4).
10. The period length, L, is determined almost solely by the refractive index, $n_s$, of the layer. This is shown best in Figure T6, which directly indicates the great dependence of the half-period thickness, L/2, on $n_s$. /379

## §3. Comparison of Measured and Calculated Curves

Figure 2 shows the measured curves obtained at three wavelengths on an evaporated layer of LiF. The multiplicity of the measurements was due to the fact that the evaporation was done in many individual steps without letting air into the vacuum (pressure $p<1\cdot10^{-5}$ Torr), with polarimetric measurement of the layer at each step.

A glance at Figures 1 and 2 shows that the experimentally determined curves have essentially the courses expected theoretically. The optically thin LiF layer on a support

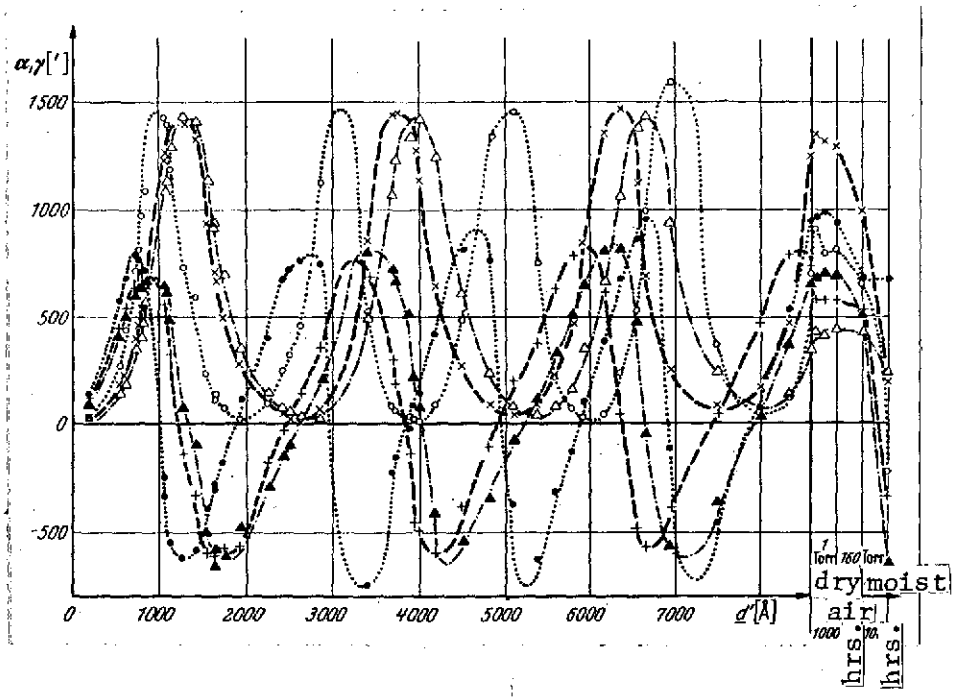


Figure 2. α and γ curves of a single LiF layer on a prism with n = 1.7234 and the action of dry and moist air at 8600 Å.

with n = 1.7234 agrees qualitatively with the calculated curve for NaCl on n = 1.7234 in Figure 1. Aside from slight discrepancies, the extremes of α coincide with the zeros for the γ curves at the same layer thickness, exactly as was discussed in §2. The requirements established in the other points of §2 are also almost quantitatively met. Therefore, we can consider that the Vasicek theory is verified. / 380

Because the period length, L, varies with differing measurement wavelength [see Equation (T4)], we can, according to the theory, determine the layer thickness, d, from the different positions of the periods for the three colors.

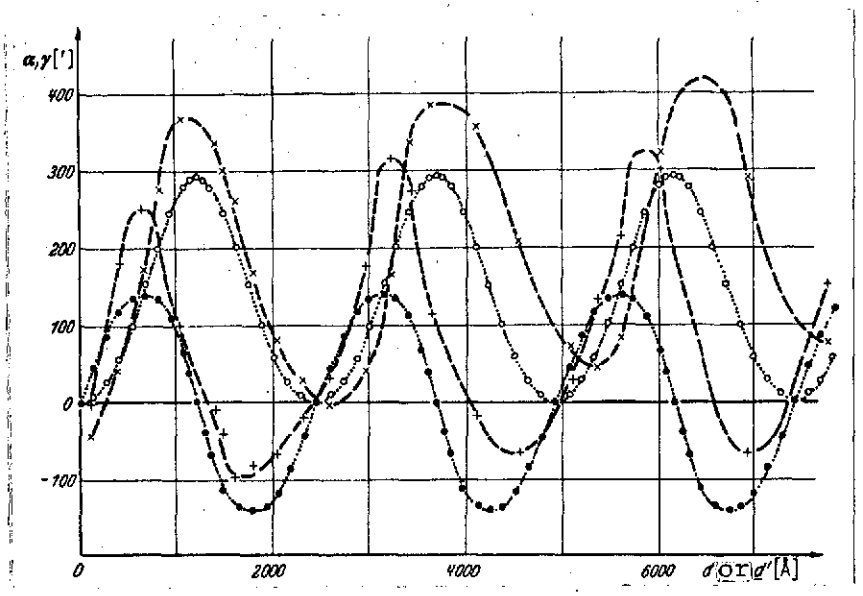


Figure 3. Theoretical (o·····o: α; •·····•: γ) and measured (×——×: α; +——+: γ) α and γ curves for single layers on prisms with n = 1.4678.

The good agreement of these thickness values, and the manner of obtaining them, are discussed in §6, using Figures 8 and 9. For most of the measured curves shown here, a mean, $\underline{d}'$, defined in §6 serves as the measure of layer thickness.

If we consider the periodic curves in Figure 2 more closely, we can see that the deviation of the α minima from zero decreases with $\underline{d}'$, and that the γ curves are unsymmetric about the zero axis. This becomes more strongly visible if we evaporate the same salt, LiF, onto a support for which the refractive index differs from that of the layer not by about 0.35, but only by about 0.08 (Figure 3). The deviations mentioned are more

noticeable. For comparison, the $\alpha$ and $\gamma$ curves calculated with the massive refractive index values according to Table 1 are plotted as dotted curves.

First, it is striking that the measured $\alpha$ maxima are higher than the theoretical ones. This has the same simple cause as the difference in the period lengths: the refractive index of the evaporated layer is less than that of the massive material. That is, the layer is somewhat porous, as is shown in more detail in §5. / 381

A more weighty point is the fact that the minima, $\alpha_n^z$ (z = number of periods), which should theoretically always be zero, become more positive from period to period. They begin with a negative value, which can be ascribed to a previous weak discharge treatment of the glass support and a transition layer with a refractive index $n_s > n$. As shown in a following publication [4], this is due to layer inhomogeneities, as are the increasing central $\gamma_n^z$ between the $\gamma$ extremes.

On the other hand, the $\alpha$ extremes match well with the appropriate $\gamma_n$ for the same layer thickness. This is almost always the case, even when the measured curves deviate severely, so that it presents the possibility for a relatively good thickness determination if L and $n_s$ are approximately known.

Cases of $n_s > n$ with the $\alpha$ curves running correspondingly entirely in the negative can also be verified in Figure 1 from the NaCl layers ($n_s$ massive = 1.547) on glasses with n = 1.4678 (Schott FK3) and n = 1.5188 (Schott BK7) [see Equation (T23)]. Figure 5 shows this with an evaporated layer of AgBr. We have essentially the dependence expected from §2 with the small deviations already discussed by means of Figures 2 and 3.

## §4. The Practical Determination of the Refractive Index $n_s$

Figure 4 shows the refractive indices determined strictly according to the procedure presented in §T5 from the $\alpha$ and $\gamma$ curves shown in Figure 2. It should not be surprising that the $n_s$ values scatter especially strongly periodically, because an exactly monoperiodic layer does not differ polarimetrically from the absence of a layer. The phase difference, $\Delta$, which is important for determination of $n_s$, arises from the relation

$$\operatorname{tg}\Delta = \mp \frac{\operatorname{tg} 2\gamma}{\sin 2\alpha} \quad \text{[see Eq. (T2)]} \qquad (1)$$

As $\alpha$ and $\gamma$ become zero for full periods, $\Delta$ must necessarily be undefined there. Because of the deviations of the $\alpha$ minima and the $\gamma_n$ values from zero, naturally large differences of the calculated $n_s$ from the massive value occur near the full periods. Thus the layer refractive indices, $n_s$, lying in the 'forbidden zones' (arbitrarily defined by $\alpha < \alpha_m/4$) which are, therefore, near the minima of $\alpha_n$, are indicated differently than the other $n_s$. The latter give better results almost throughout. That is, they are nearer the best values defined in the following. This gives rise to the conjecture that the best $n_s$ value can be obtained from the maximum, $\alpha_m$, if the matching $\gamma_n$, even if it differs somewhat from zero, contrary to the theory, has hardly any effect on the magnitude of $|\psi_{max}|$ and $n_s$, according to the equation

/ 382

$$\cos 2\psi = \cos 2\alpha \cdot \cos 2\gamma \quad \text{[see Eq. (T1)]} \qquad (2)$$

(see Figure T9). The values thus obtained are taken as constant for the whole period and called the best values, $n_s^z$. They are

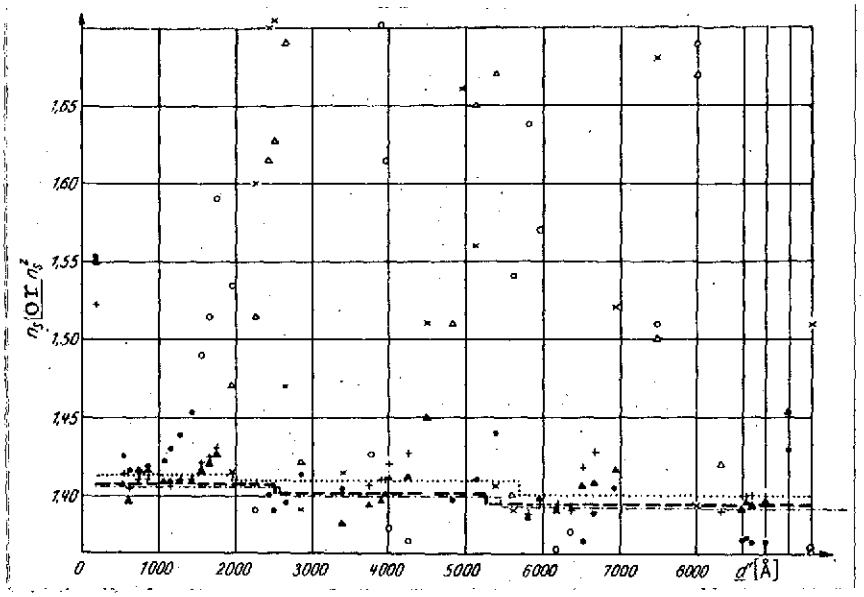


Figure 4. Measured refractive indices, $n_s$, and the best values, $n_s^z$, for the LiF layer of Figure 2 on a prism with $n^s = 1.7234$. $\alpha > \frac{\alpha_{max}}{4}$ {+++: $\lambda = 5461$ Å; ●●●: $\lambda = 4358$ Å; ▲▲▲: $\lambda = 5780$ Å; $\alpha < \frac{\alpha_{max}}{4}$ {×××: $\lambda = 5461$ Å; ○○○: $\lambda = 4358$ Å; △△△: $\lambda = 5780$ Å; $n_s^z$ {– – –: $\lambda = 5461$ Å; ·····: $\lambda = 4358$ Å; –·–: $\lambda = 5780$ Å

shown by the horizontal lines in Figure 4 *.

Measurement with three frequencies proves to be a great advantage here. The 'forbidden zones' with $\alpha < \alpha_m/4$ appear at different layer thicknesses for each color, so that refractive index determinations are practically always possible within /383
the limits of error, from the curve, for two or at least one wavelength, even without knowledge of an $\alpha_m$ with the resulting best value $n_s^z$.

---

* The best values, $n_s^z$, for most of the substances measured by the author are below the massive values of Table 1 because of weak porosity of the layers (see Table 2). Upward deviations can be explained as a double layer effect on the basis of natural transition layers of the support glass. Almost complete elimination of the effects of these transition layers is made possible by means of the inhomogeneity rules in the following publication [3] on inhomogeneous layers.

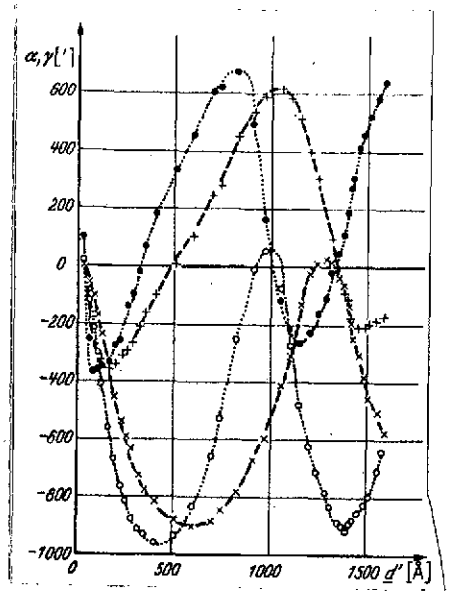


Figure 5. α and γ curves for a single layer of AgBr on a prism with n = 1.7234.

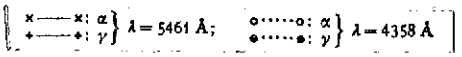


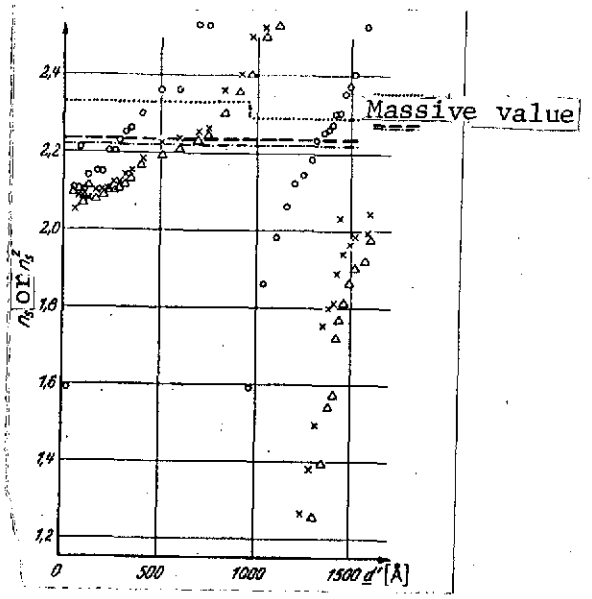


Figure 6. Measured refractive indices, $n_s$ and best values of the reflective index, $n_s^z$, for AgBr on a prism with n = 1.7234.

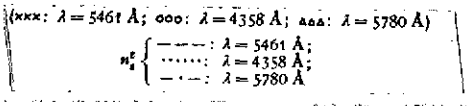


Figures 5 and 6 show the causes of the false determination of refractive index in the 'forbidden zones' particularly well: The shift of the zero values of $\alpha_n$ and $\gamma_n$ toward positive values gives excessively large Δ to the left of $\alpha_n$ [see Equation (1)] because the γ values are too great and the α values are near zero for too long because of the shift of $\alpha_n$ toward the positive, so that they are too small. But, according to Figure T3, an excessively large Δ at relatively high $\psi$ immediately yields too high values of $n_s$, especially because of the flatness of the phase difference curves in this region. Also, the change of sign of α causes a physically unmotivated jump of $n_s$ to values smaller than n.

The converse is true for the right side of an $\alpha_n$ point. At first $|\gamma|$ decreases, instead of increasing according to §2.3, and it remains above the corresponding values in the first half-period, so that $\Delta$ and $n_s$ become too small.

## §5. The Effect of the Rate of Evaporation

/384

In this relation, we must refer to a phenomenon which appeared with LiF evaporation. Figure 7a shows, in a $n_s$-$\underline{d}$ diagram, the continuous transition of $n_s$ from the value of n for glass at $\underline{d} \approx 0$ through the measured value for the transition layer to that of the evaporated substance. The quantity $\underline{d}$ is defined in the next paragraph.

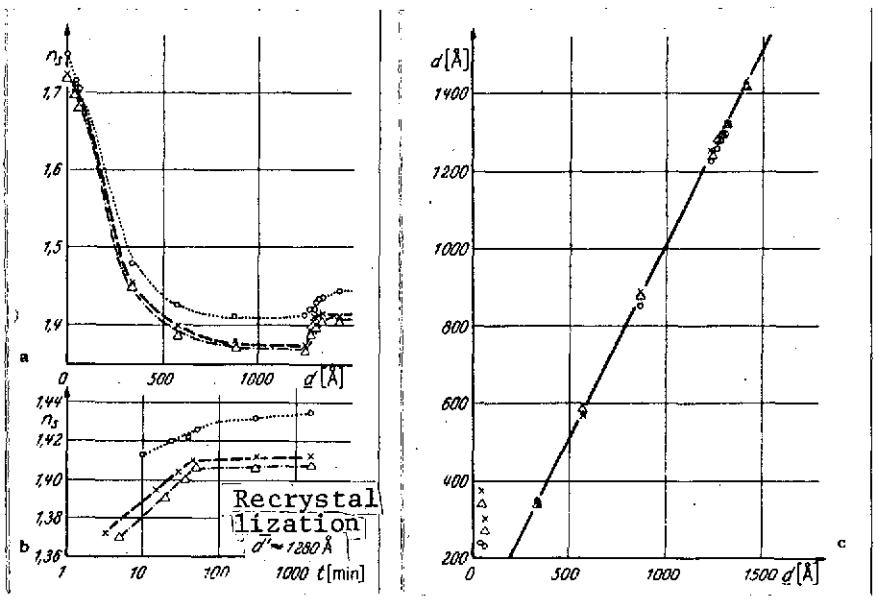


Figure 7 a-c. Single layer of LiF on a prism of n = 1.7234. n = 1,7234. ×××: λ = 5461 Å; ooo: λ = 4358 Å; ΔΔΔ: λ = 5780 Å. a) Change of the measured value of refractive index, $n_s$, with increasing thickness of an evaporated LiF layer. b) Change in refractive index of a rapidly evaporated LiF layer at room temperature in vacuo. c) Explanation in §6.

As the layer from 860 to 1240 Å in particular was applied quite rapidly, the value for $n_s$ was extremely low. This, no doubt, like the neighboring values, really indicates at least the relative change, as it could be obtained almost exactly at the maximum, $\alpha_m$. The points following the value at 1240 Å were maintained by no additional evaporation up to 1330 Å, but in the course of 1,000 minutes on the same layer ($n_s$-t curve in Figure 7b). The $n_s$ values for all three colors at first rise on a logarithmic time scale approximately linearly, and then approach saturation.

This phenomenon, appearing just with LiF after rapid evaporation, strongly suggests recrystallization. This agrees with the observations of Road [5], who established first a porosity and then a slowing change with time, through intensity measurements on evaporated layers. / 385

## §6. The Practical Determination of the Layer Thickness

We must first illuminate the concept of the layer thickness in somewhat more detail. The Vasicek theory [1, 2] generally yields very high layer thicknesses for $n_s \approx n$ (see Figures T6 and T7), because here the entire zone also shows the lowest deviation of the refractive index from the massive value. Now if one deposits a layer with a greatly different $n_s$, we have a double layer [4], for which the first layer ($n_s \approx n$) can hardly be differentiated any more from the support. Now, with d, we measure predominantly the thickness of the second evaporated layer. In spite of a continuous increase in the total thickness, strictly considered, in the growth, the measured thickness will first drop significantly, along with a strong change of $n_s$. This phenomenon is particularly well visible in the d-d diagram in Figure 7c. Here, the values, d, always determined from the theory with the matching $n_s$, are

plotted versus the d triplet corresponding to the mean $\underline{d}$ for the three wavelengths. The only exception is for the disproportionately high initial thicknesses of the transition layer, which are plotted in this case at one value of $\underline{d}$, determined from the $n_s$-$\underline{d}$ diagram of Figure 7a by free arrangement of the $n_s$ values for the transition layer on the curve.

Figure 8 reproduces the layer thicknesses, d, already shown for the LiF layer in Figure 2, based on the matching refractive indices according to Figure 4. The thick curve is the theoretical 100% line, while the thin dashed lines indicate the 5% limits of error. Here, too, as in Figure 4, some thickness values are periodically missing completely in succession for the three colors because of the use of the $n_s$ from the 'forbidden zones'. The d' values are arranged decisively better in Figure 9, for greater thicknesses and within a 1% error limit. Thus we define: $\underline{d}'$ are the means of the d' triplet obtained for the three measuring wavelengths, on the basis of the best value, $n_s^z$.

It is noteworthy how well the d' triplets coincide according to Figure 9 and also in other cases with considerably larger regular deviations of the $\alpha$ and $\gamma$ curves, although the thickness values were obtained from quite different period positions for the three colors.

The accuracy with which the thickness changes can be established directly optically is considerable in favorable cases. In the case of Figure 2, for instance, $\alpha_m^1 = 1410'$ at / 386
a half-period length of L/2 = 1250 Å. For an $\alpha$-reading accuracy at a single setting, which varies by 10', depending on the value / 387
of $\gamma'$, the detectable thickness change in the most favorable range between 750 and 1000 Å at $\partial\alpha/\partial d \approx 3\,['/\text{Å}]$ is certainly less than 10 Å. For any thickness greater than about 20% of the period

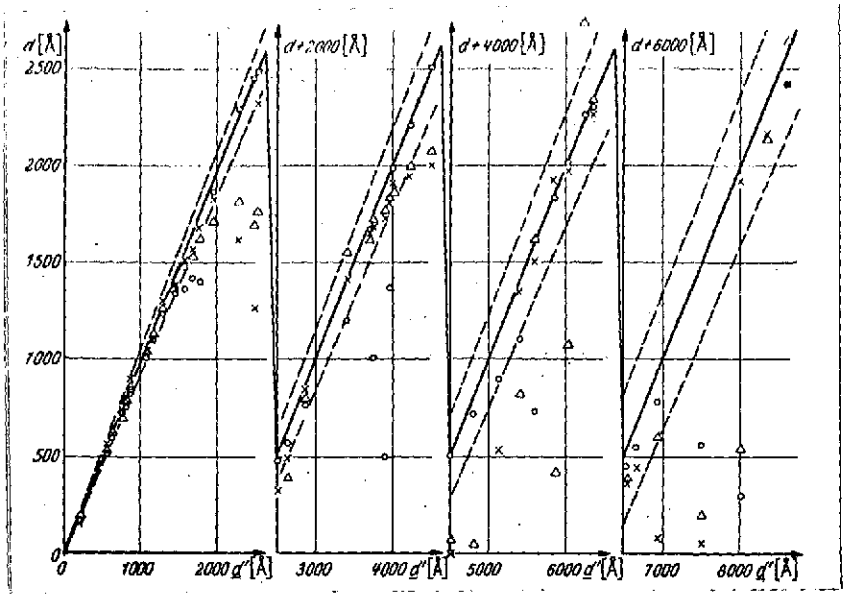


Figure 8. Layer thicknesses d, calculated with the matching measured refractive indices, $n_s$, for the LiF layer of Figures 2 and 4 on a prism with n = 1.7234.

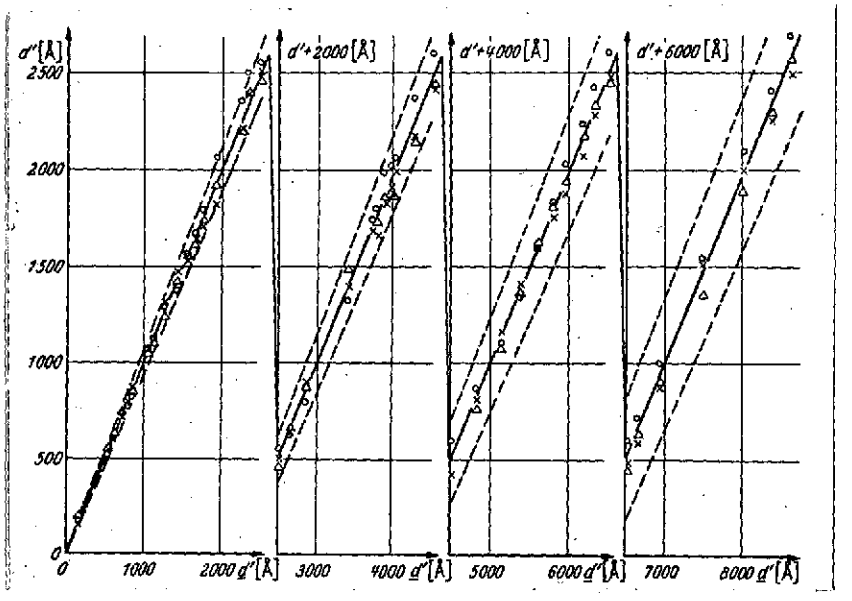


Figure 9. Layer thicknesses, d', calculated with the best values, $n_s^z$ of the measured refractive indices $n_s$ for the LiF layer according to Figures 2 and 4 on a prism with n = 1.7234.

length, L, one can obtain such a favorable derivative by choice of the wavelength.

## §7. The Tempering of Evaporated Layers in Vacuum and the Action of Moist Room Air

In the tempering of a layer 7700 Å thick in vacuum, it appeared that the α and γ curves appear toward lower layer thicknesses. This is coupled with a change in the extreme value heights. Thus, formal application of the Vasicek theory yields layer thicknesses decreased to 7000 Å at 400°C, and which remain approximately constant on further temperature rise to 700°C.

Quite different extreme value heights appeared for different colors before tempering. This is a typical effect produced by access of air to a multiple layer [4]. Conversely, the fact that vacuum tempering again levels off the extremes of different colors indicates compensation of the step in refractive index caused by the access of air, i.e., a homogenization of the layer.

Action of air, like tempering, causes a short regression of the curves. This effect occurs primarily with moist air (see Figure 2) so that the explanation must be sought largely in the action of water alone.

Without covering the conclusions from many investigated layers in detail here, it may be said that all the polarimetric phenomena can be satisfactorily explained only by assuming that humidity increases the refractive index, with simultaneous shrinkage of the layer thickness. In agreement with observations by Koppelmann, Krebs and Leyendecker [6], the effects of uptake of moisture cannot be explained by simple double layer

inhomogeneity. Rather, considerably more complex changes occur in the layers. It has not yet been possible to understand them. One proof of this is the often-observed deterioration of the γ curves after particularly protracted air access. In contrast to all observations on artificial double layers [4], this deterioration consists of a period height completely contradicting the requirement of §2.5 (see Table D3, LiF layer III on a prism with n = 1.6262).

The fact that a notably good layer thickness assignment was obtained even with the thickest layer investigated by the author (22,200 Å) in spite of this deterioration, even on the basis of the best value, $n_s^z$, determined strictly according to §4, is shown by the comparison with the interference /388
microscopic results in Table 2 (LiF layer on a prism with n = 1.6262). The clear course of the curve shows that the Vasicek theory is applicable throughout, even up to large layer thicknesses. The deterioration after the action of air does not limit it in any way, as it is constant and apparently due to a sudden change of the lower layer through the action of humidity.

## §8. The Evaporation of NaCl and LiCl

For testing the Vasicek theory, we considered only materials crystallizing in the cubic pattern (i. e., isotropic materials). They should show no aging phenomena or susceptibility to trouble, as much as possible, and should meet the requirement for refractive index range. With LiF and the silver salts, AgCl and AgBr, we have available substances with $n_s$ smaller (LiF) or greater (AgCl, AgBr) than all support refractive indices n. The silver salts proved to be surprisingly constant in their optical properties when the vacuum apparatus was sealed light-tight and the action of the

measuring light was kept as brief as possible. However, it was interesting, and necessary for the double layer model to be discussed later [4] to have a cubically crystallizing material which had $n_s \gtrless n$, depending on the support refractive index. In the final choice there remained only NaBr, LiCl and NaCl; but all of them had the disadvantage of high solubility in water. Access of air caused droplet formation and disappearance of the interference colors in seconds with LiCl and in minutes with NaBr. Unfortunately, these effects also occurred with NaCl, although to a somewhat lesser extent. Severe aging phenomena appear even in vacuum (pressure, $p < 1 \cdot 10^{-5}$ Torr). Even when working as fast as possible, there appeared large measurements (Figure 10b) which apparently deviated fundamentally from the theoretical curves (Figure 10a). We can say nothing more of the $\alpha_n$ and $\gamma_n$ null values without more information. In contrast, the $\alpha$ and $\gamma$ curves diverge entirely and never intersect.

The theoretical curves from Figure 1 and the measurements obtained with essentially homogeneous layers let a decision between $\alpha$ maxima and minima appear obvious: $|\alpha_m|$ must be larger than $|\alpha_n|$. If we try to work similarly for the NaCl layers, we find ourselves in a contradiction. The solution of this problem involved the decisive ideas for unification of the concept and for explanation of the inhomogeneity phenomena [4].

The distance from zero of the opposing $\alpha$ extremes in Figure 10b changes strongly with d", although the measurements with NaCl on glasses with n = 1.7234 (see Figure D8 and D9) show that measurable layers are formed throughout. /389
Thus, the effect of the increase in $\alpha_n^z$ (see §3) which was only weak there must have produced this grotesque-appearing deterioration with the NaCl layers on n = 1.4678 and n = 1.5188. Apparently only the beginning of the $\alpha$ curve approximately

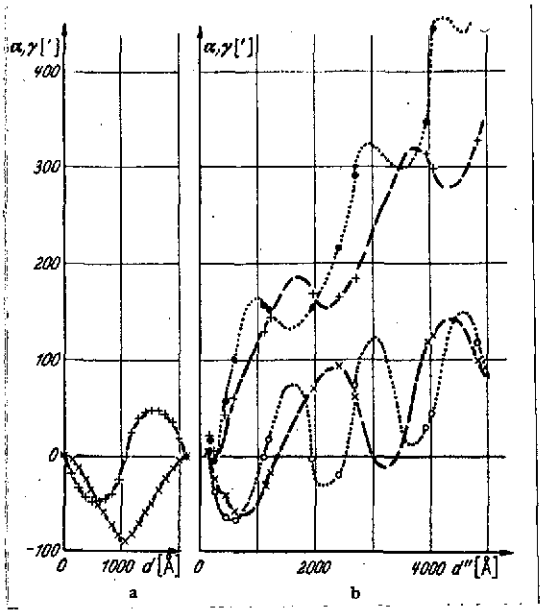


Figure 10 a and b. α and γ curves for a single NaCl layer on prisms with n = 1.5188.
a: theoretical; b: measured.

matches the theoretical course according to Figure 10a. Thus, only this can affect the decision between the $\alpha_m$ and $\alpha_n$.

Therefore, we define for all further applications: $\alpha_m^1$ is the first extreme of α after the beginning of layer formation; and $\alpha_n^2$ is the following opposite α extreme. Then the $\alpha_m^z$ and $\alpha_n^z$ values for the periods, z, appear alternately.

With these definitions, we see that in Figure 10b we have only an enlargement of the increase of $\alpha_n$ and $\gamma_n$ which we already observed in Figure 2, while the basic curve shape remains the same except for an additive component increasing approximately linearly with d''. We also see the important coincidence of the α extreme points with the matching mean $\gamma_n$ for the γ extremes at the same thickness.

The drawing of Figure 10b and corresponding other $\alpha$ and $\gamma$ curves for NaCl and LiCl layers, for which data are presented in Table 2, presented considerable difficulties, though, because modified application of the Vasicek theory according to §6 was impossible.

## §9. Determination of Thickness for Severely Inhomogeneous Layers

With the abnormal behavior of the measurements in Figure 10b, only an empirical method simultaneously representing the only possibility for thickness determination with double layer models could lead to the goal.

The most important quantities are the period lengths, L, calculated in Figure 10b from those best values, $n_s^1$, of the curves which corresponded to the $\alpha_m^1$. With the double layers [4], L was matched to the corresponding lengths for comparable single layers. With entirely unknown layers, therefore, a value of $n_s$ determined from polarimetric data or other considerations must be used as a basis for the calculation of L.

Once one has obtained this period length, then the separation of successive extremes of $\alpha_n$ or $\alpha_m$, equal to L, is established. Now the other measurements for a period are assigned by empirical shifting so that the resulting curve shapes match the theory as well as possible. There is a decisive secondary condition which is an important help, especially with lacking $\alpha_n$ and, thus, doubtful assignments to the individual periods: this is that similar curves appear simultaneously for all three measuring wavelengths. The layer thicknesses determined in this way were designated as d".

Table 2. BEST VALUES OF REFRACTIVE INDEX, $n_s^z$, AND LAYER THICKNESSES DETERMINED BY POLARIMETRY INTERFERENCE MICROSCOPY.

g: $\lambda = 5461$ Å; ge: $\lambda = 5780$ Å; b: $\lambda = 4358$ Å;
n = support refractive index for $\lambda$ = 5461 Å.
u = unignited; gl = ignited.

| Fig. Nr. | Name | n | Salt | Type | z | $n^z_{sg}$ | $n^z_{sge}$ | $n^z_{sb}$ | $d_{pol}$ [Å] | $d_{int}$ [Å] |
|---|---|---|---|---|---|---|---|---|---|---|
| 3 | FK3 | 1,4678 | LiF | gl | 1 | 1,379 | 1,378 | 1,387 | 7860 | 7600 |
| | | | | | 2 | 1,373 | 1,372 | 1,376 | | |
| | | | | | 3 | 1,368 | 1,367 | 1,369 | | |
| I | BK7 | 1,5188 | LiF | u | 1 | 1,406 | 1,405 | 1,413 | 9400 | 9000 |
| | | | | | 2 | 1,395 | 1,393 | 1,404 | | |
| | | | | | 3 | 1,395 | 1,393 | 1,397 | | |
| | | | | | 4 | 1,395 | 1,393 | 1,397 | | |
| II | SK10 | 1,6262 | LiF | u | 1 | 1,395 | 1,393 | 1,399 | 7100 | 7200 |
| III | SK10 | 1,6262 | LiF | u | 1 | 1,382 | 1,381 | 1,392 | 10000 | 9700 |
| | | | | | 2 | 1,374 | 1,381 | 1,388 | 22200 | 21800 |
| | | | | | 3 | 1,370 | 1,378 | 1,390 | | |
| | | | | | 4 | | | 1,390 | | |
| 2 | SF1 | 1,7234 | LiF | u | 1 | 1,407 | 1,406 | 1,413 | 8600 | |
| | | | | | 2 | 1,401 | 1,400 | 1,409 | | |
| | | | | | 3 | 1,393 | 1,392 | 1,402 | | |
| | | | | | 4 | 1,390 | 1,389 | 1,394 | | |
| | | | | | 5 | | | 1,392 | | |
| D6[4] | FK3 | 1,4678 | NaCl | u | 1 | 1,548 | 1,546 | 1,556 | 5500 | 4600 |
| | | | | | 2 | 1,520 | 1,518 | 1,530 | | |
| | | | | | 3 | 1,502 | 1,500 | 1,512 | | |
| D7[4] | FK3 | 1,4678 | NaCl | gl | 1 | 1,510 | 1,508 | 1,526 | 5500 | 5400 |
| | | | | | 2 | 1,498 | 1,498 | 1,513 | | |
| | | | | | 3 | 1,496 | 1,490 | 1,504 | | |
| IV | BK7 | 1,5188 | NaCl | u | 1 | 1,540 | 1,537 | 1,548 | 3900 | 3600 |
| | | | | | 2 | 1,520 | 1,516 | 1,526 | | |
| | | | | | 3 | | | 1,508 | | |
| 10b | BK7 | 1,5188 | NaCl | u | 1 | 1,540 | 1,538 | 1,549 | 4800 | 4800 |
| | | | | | 2 | 1,523 | 1,520 | 1,535 | | |
| | | | | | 3 | | | 1,514 | | |
| D8[4] | SF1 | 1,7234 | NaCl | u | 1 | 1,527 | 1,523 | 1,547 | 6750 | |
| | | | | | 2 | 1,522 | 1,520 | 1,540 | | |
| | | | | | 3 | 1,502 | 1,499 | 1,510 | | |
| | | | | | 4 | | | 1,506 | | |
| D9[4] | SF1 | 1,7234 | NaCl | gl | 1 | 1,498 | 1,497 | 1,516 | 7000 | |
| | | | | | 2 | 1,478 | 1,476 | 1,480 | | |
| | | | | | 3 | 1,460 | 1,459 | 1,464 | | |
| | | | | | 4 | | | 1,452 | | |
| V | BK7 | 1,5188 | LiCl | u | 1 | 1,612 | | 1,628 | 5700 | |
| | | | | | 2 | 1,592 | | 1,613 | | |
| | | | | | 3 | 1,557 | | 1,588 | | |
| | | | | | 4 | 1,526 | | 1,530 | | |
| VI | FK3 | 1,4678 | AgCl | gl | 1 | 2,026 | 2,024 | 2,040 | 2130 | 2150 |
| | | | | | 2 | | | 2,020 | | |
| VII | FK3 | 1,4678 | AgCl | gl | 1 | 2,036 | 2,028 | 2,020 | 2180 | 2150 |
| | | | | | 2 | 2,042 | 2,036 | 2,030 | | |
| VIII | FK3 | 1,4678 | AgCl | gl | 1 | 2,048 | 2,040 | 2,050 | 2200 | |
| | | | | | 2 | 2,042 | 2,038 | 2,050 | | |
| IX | BK7 | 1,5188 | AgCl | u | 1 | 1,952 | 1,952 | 1,976 | 3040 | 3000 |
| | | | | | 2 | 1,952 | 1,952 | 1,950 | | |
| X | SF1 | 1,7234 | AgCl | u | 1 | 2,036 | 2,028 | 2,072 | 2750 | 2700 |
| | | | | | 2 | 2,054 | 2,048 | 2,082 | | |
| 5 | SF1 | 1,7234 | AgBr | u | 1 | 2,233 | 2,220 | 2,330 | 1580 | 1500 |
| | | | | | 2 | | | 2,286 | | |

Here, as also with all uninterrupted evaporations of layers with more than a period thickness without continuous observation, use of different measuring frequencies is the sole criterion for deciding on the number of periods.

The polarimetric method, however, without added experimental problems, is suited to immediate observation of the following quantities:

1. the period number, z;
2. the height of the decisive $\alpha_m^z$ for the best value, $n_s^z$;
3. the decisive $\alpha_n^z$ for the period length with inhomogeneous layers;
4. attainment of a desired layer thickness when the curve shape is known from preliminary experiments

during a slow vapor deposition by optically following the change of the azimuth, $\alpha$ for one wavelength.

## §10. The Best Value of Refractive Index, $n_s^z$, of the Layers Investigated and Comparison of the Layer Thicknesses Obtained by Polarimetry and Interference Microscopy.

In the following, the best values of refractive index for all the single layers studied are presented in Table 2.

The total layer thicknesses determined by polarimetry and interference microscopy appear in two other columns. In order to insure the independence of the two methods, the results from one method were always evaluated without knowledge of the results from the other. It should also be noted that in the normalized Vasicek method [1] we work below the polarization angle, $\varphi_P$, of the support; that we work with normal incidence of light in interference microscopy; and that in the former we measure primarily $n_s \cdot d$ and in the latter, d alone. /392

As Table 2 shows, the layer thicknesses agree practically within the limits of error.

The relatively great differences of the $n_s^z$ values, with NaCl layers, for instance, are due mainly to the different surface nature of the glass support. In the following publication they can be explained as a double layer effect from inhomogeneous layers, and almost quantitatively eliminated.

I thank Prof. Dr. Eugen Kappler for his stimulating interest and for his provision of the means to perform this work.

REFERENCES

1. Rassow, J. Called briefly "Part I" in the following. Figures and equations from this reference are prefixed with the letter T. Z. Physik, Vol. 168, 1962, p. 353.

2. Vasicek, A. J. Opt. Soc. Amer. Vol. 37, 1947, p. 145.

3. Vasicek, A. J. Opt. Soc. Amer. Vol. 37, 1947, p. 979.

4. Rassow, J. The figures on double evaporated layers from this work are prefixed with the letter D. Z. Physik, Vol. 170, 1962, p. 393.

5. Road, J. L. J. Opt. Soc. Amer. Vol. 39, 1949, p. 854.

6. Koppelmann, G., K. Krebs and H. Leyendecker. Z. Physik, Vol. 163, 1961, p. 567.